HEAD & NECK IMAGING

Iran J Radiol. 2020 July; 17(3):e99924. doi: 10.5812/iranjradiol.99924.

Published online 2020 June 24. **Research Article**

Diagnostic Value of Dual-Energy CT Iodine for Characterization of Papillary Thyroid Microcarcinoma and Better Prediction of Metastatic Cervical Lymph Nodes

YI-Long Huang [1], Yuan-Ming Jiang [1], Zheng-Hua Zhang [1], Wen Zhao [1], Yue Jiang [2], Yang Lin [3], Bo He [1] and Dan Han [1, *]

[1] Department of Radiology, The First Affiliated Hospital of Kunming Medical University, Kunming, China
[2] Department of Radiology, Yan' An Hospital of Kunming Medical University, Kunming, China
[3] Department of Diagnostic Imaging, Siemens Healthcare, Shanghai, China

[*] *Corresponding author*: The First Affiliated Hospital of Kunming Medical University Kunming, China. Email: kmhandan@sina.com

Received 2019 December 10; **Revised** 2020 May 19; **Accepted** 2020 May 26.

Abstract

Background: The preoperative assessment of cervical lymph node metastasis (LNM) is considered a challenging clinical problem in papillary thyroid microcarcinoma (PTMC) patients. Ultrasonic examination is significant for the cervical LNM in PTMC patients, but there are difficulties and limitations in observing lymph nodes in the cervical central region.
Objectives: To investigate the diagnostic value of dual-energy computed tomography (DECT) iodine for characterization of PTMC and better prediction of metastatic cervical lymph nodes of PTMC.
Patients and Methods: Ninety-five patients with PTMC who underwent DECT examinations were retrospectively enrolled in the study. The iodine image morphological features of primary tumor were analyzed in the arterial phase and quantitative DECT parameters of the primary tumor were recorded in the arterial and venous phase. Chi-square test and independent-sample t test were performed to compare the differences of morphological features and quantitative parameters of tumors between LNM and non-LNM groups. Receiver operating characteristic curves were generated to assess the diagnostic performance of each DECT parameter and their combinations.
Results: Six primary tumor morphological features of the LNM group demonstrated significant differences compared with the non-LNM group (all $p < 0.05$). Normalized iodine concentration (NIC) and normalized CT value in the LNM group were significantly higher than those of the non-LNM group in both arterial and venous phase, respectively (all $p < 0.001$). The area under the curve (AUC) was improved from 0.814 to 0.843 after adding maximum diameter compared with incomplete thyroid capsule alone. In addition, the combination of NICs in arterial and venous phases had higher AUC than other quantitative parameters.
Conclusion: Morphological features and quantitative parameters of DECT are valuable for predicting cervical LNM in patients with PTMC.

Keywords: Tomography, X-Ray Computed, Iodine, Lymph Node, Neoplasm Metastasis

1. Background

Papillary thyroid carcinoma (PTC) is the most frequently malignant tumor of the thyroid gland. The incidence of PTC has increased rapidly worldwide in the recent years, mainly because of the early detection of papillary thyroid microcarcinoma (PTMC), which is defined as PTC $\leq$ 1 cm in the greatest dimension (1). PTMC has a relatively good prognosis, with a high survival rate and low recurrence rate. However, the treatment of patients with PTMC is controversial. Studies by Pacini (2) and Zhang et al. (3) showed that PTMC had all the biological characteristics of malignant tumors and the lymph node metastasis (LNM) rate was up to 50% with the main predictors of invasion, recurrence, and distant metastases. The 2015 guidelines of the American Thyroid Association do not recommend cervical lymph node dissection (LND) in PTMC patients without clear evidence of existing LNM (4, 5). At present, whether PTMC patients need thyroidectomy or cervical LND depends on the occurrence of cervical LNM. Some studies have predicted the LNM by clinical and pathologic features, but the results were varied, and further investigation is warranted (3, 6, 7). Ultrasonic examination is significant for the preoperative diagnosis of cervical LNM in PTMC patients; however, it has difficulties and limitations for observing the lymph node at the cervical central

region. Several studies have found that dual-energy computed tomography (DECT) is prior to conventional CT in visualizing the morphological edge and internal structure of lesions, and the iodine image obtained from DECT is helpful in differential diagnosis of benign and malignant thyroid nodules (8, 9).

2. Objectives

The aim of this retrospective study was to provide new evidence for characterization of PTMC and better prediction of metastatic cervical lymph nodes in PTMC patients with DECT.

3. Patients and Methods

3.1. Patients

This retrospective study was approved by our institutional review board and patient consent was waived. All neck DECT examinations performed between January 2013 and June 2018 were retrospectively reviewed. A radiologist who had access to complete patient files, including clinical, surgical, histopathological data and ultrasound results, as well as CT reports, reviewed the DECTs of PTMC patients with pathological nodes, either LNM or non-LNM in the neck. Tissue diagnosis and interpretation were based on the 2015 guidelines of the American Thyroid Association (4). The selection process for PTMC patients is shown in Figure 1. Finally, a total of ninety-five PTMC patients (24 men, 71 women; average age of 43.32 ± 11.34 years; LNM, n = 59; non-LNM, n = 36) were included in the study. And the number of subclinical LNM cases diagnosed by ultrasound was only 7, but ultrasound results showed cervical lymphadenopathy in 23 of non-LNM cases. All patients were from southwest China (most of the patients were from Yunnan Province) and received primary treatment in our hospital.

3.2. Dual-Energy CT Scan Protocol

All CT scans were performed on a second-generation 128-section dual-source CT scanner (SOMATOM Definition Flash; Siemens Healthcare, Forchheim, Germany). The DECT protocol was as follows: tube A, 80 kVp, reference current time product of 150 mAs per rotation; tube B, Sn140 kVp with tin filter, automatic tube current. Dedicated tube current-modulation software (CARE Dose 4D, Siemens Healthcare) automatically set the tube current in real time to reduce the radiation dose. Additional parameters were: 128×0.6 mm collimation, 0.28 s rotation time, 0.7 pitch, 0.75 mm slice thickness, 0.50 mm slice increment, linear blended M = 0.5, and convolution kernel D30f. Contrast medium (iopromide injection, 370 mgI/mL, Bayer Healthcare, Germany) was injected through an antecubital vein at a flow rate of 3 mL/s with a total amount of 65 mL. The test bolus technique was used to determine the scan delay time. The aortic arch was selected as the monitoring level, and 100 Hounsfield unit (HU) was selected as the trigger threshold. The delay time of arterial phase was 5 s after injection, and venous phase was 25 s later. DECT examination has radiation risks, but we monitored radiation for each patient and followed the criteria of as low as reasonably achievable.

3.3. Analysis of Morphological Features and Quantitative Parameters in Iodine Images

The dual-energy data of arterial and venous phases were loaded into a dual-energy virtual non-contrast (VNC) application software package (Multi-Modality Workplace 70212, Siemens Healthcare, Forchheim, Germany). The analysis of PTMC morphological features and measurement of quantitative parameters were performed by two senior radiologists with 10 years of experience in head and neck radiology. The radiologists focused only on tumor and were blind about clinical information and pathological results of LNM. The final diagnosis was arrived at by consensus. PTMC morphological features of primary lesions were analysed in the arterial phase, including multiple lesions (number of lesions > 1, and located lesions based on pathological findings), maximum diameter of nodule > 5.0 mm, aspect ratio > 1 (the anteroposterior and transverse diameter ratio [A/T] on axial view), irregular shape, incomplete nodule enhanced ring (i.e. enhanced ring of PTMC nodular is incomplete), incomplete thyroid capsule (i.e. defined as the imaging findings of PTMC invasion outside the thyroid capsule), microcalcification (calcification with diameter < 2.0 mm), and enhanced degree of the region of interest (ROI) in arterial phase (mild and moderate enhancement when the net increased CT value was $\leq$ 40 HU, and significant enhancement when it was > 40 HU) (10).

Iodine concentration (IC) and CT value of the arterial and venous phase were measured separately at the solid components of PTMC and ipsilateral internal carotid artery by placing ROIs at the same slice in the largest cross-sectional area of the lesions, and carefully avoiding calcification and necrosis. The accurate tumor location information was based on pathological results. Cases with unclear solid component of the lesion were excluded. ROIs accounted for 70% to 80% of the total area of the PTMC solid components at the largest level. All measurements were performed three times by the two above-mentioned radiologists and the average values were calculated. In addition, normalized IC (NIC) and CT value were calculated as follows: $NIC = IC_{ROI}/IC_{\text{internal carotid artery}}$; normalized CT value = $CT_{ROI}/CT_{\text{internal carotid artery}}$.

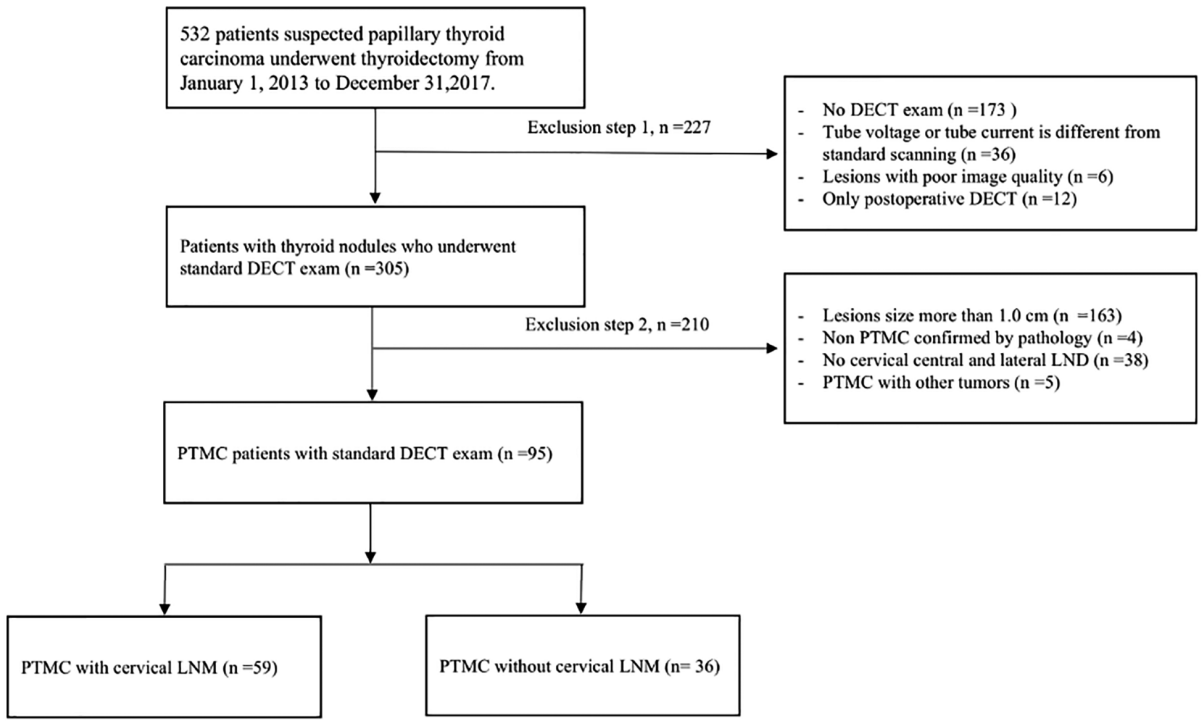

Figure 1. Selection process for papillary thyroid microcarcinoma (PTMC) patients in this retrospective study

3.4. Statistical Analysis

All analyses were performed using the statistical software SPSS® II for Windows v. 22.0 (IBM SPSS Inc., Chicago, IL, USA). A P value < 0.05 was considered to indicate a significant difference. All measured values were expressed as mean $\pm$ standard deviation. Chi-square and Fisher exact tests were used for categorical data. The Spearman's rank correlation analysis was used to evaluate the correlation between iodine image morphological features in primary lesions and cervical LNM in patients with PTMC. An independent two-sample t test was used to compare the differences of six quantitative parameters between the LNM group and the non-LNM group in both arterial and venous phases. In addition, diagnostic efficiency of various DECT parameters was evaluated and compared using receiver-operating characteristic (ROC) curves analysis.

4. Results

4.1. Association of Morphological Features with Cervical LNM in Iodine Image

The boundary and internal structure of PTMC in iodine images were more clear than those in the linear blending images (Figure 2A-C and Figure 3A-D). Incomplete thyroid capsule (Figure 2D and Figure 3D), multiple round low-density nodules, and blurred edge in the thyroid (Figure 2C) could be shown in the iodine images. Table 1 demonstrates the correlation between morphological features and cervical LNM. Six features of the iodine image were significantly related to cervical LNM: multiple lesion, maximum diameter > 5 mm, aspect ratio > 1, irregular shape, incomplete nodule enhanced ring, and incomplete thyroid capsule. Microcalcification and enhanced degree were not significantly related to the presence of cervical LNM. The correlation rank was as follows: incomplete thyroid capsule (r = 0.495), multiple lesion (r = 0.397), "aspect ratio > 1" (r = 0.348), irregular shape maximum (r = 0.309), "maximum diameter > 5 mm" (r = 0.303), incomplete nodule enhanced ring (r = 0.258) (Table 1). Diagnostic efficiency of morphological features for prediction of LNM is provided in Table 2. The sign of incomplete thyroid capsule in primary lesions had the highest diagnostic efficiency for the potential of LNM: sensitivity = 77.97%, specificity = 72.22%, accuracy = 75.79%, AUC = 0.757. After combining two significant morphological features, the sensitivity was significantly increased, but the specificity decreased. Combination of incomplete thyroid capsule and "maximum diameter > 5 mm" had the highest diagnostic effi-

ciency among all parameters. AUC of this combination was higher than that of alone incomplete thyroid capsule and "maximum diameter > 5 mm" (Table 3).

4.2. Differences in DECT Quantitative Parameters between LNM and Non-LNM Groups

Comparisons of ICROI, IC internal carotid artery, NIC, CT value ROI, CT value internal carotid artery, and normalized CT value in the arterial and venous phases are shown in Figure 4A-F. No significant difference was found in ICROI, IC internal carotid artery, CT value ROI, or CT value internal carotid artery between LNM group and non-LNM group (all Ps $\geq$ 0.05). However, the NIC and normalized CT value of the LNM group were statistically higher than those of the non-LNM group in both phases (all Ps < 0.05).

4.3. Diagnostic Efficacy of Alone and Combined DECT Quantitative Parameters

ROC curve was drawn to compare the comprehensive diagnostic efficiencies of the four statistically significant quantitative parameters (Figure 5A). The ROC curve analysis found that the AUC of the NIC in the arterial phase was the highest, with an area under the ROC curve of 0.814. Taking 0.208 as the threshold, the sensitivity was 73.50% and the specificity was 79.20%. The diagnostic efficiency rank of AUC was NIC in the arterial phase, NIC in the venous phase, normalized CT value in the arterial phase, and normalized CT value in the venous phase. Figure 2E-H and Figure 3E-H showed the NIC of iodine image in a PTMC patient with cervical LNM and their pathological results. After combining two parameters separately in four significant parameters and comparing their ROCs, the combination of NICs in the arterial and venous has higher diagnostic efficiencies and AUC (0.843) than the other combinations (Figure 4B).

5. Discussion

Ultrasound is the most commonly used imaging examination for diagnosis of PTMC. The advantage of CT examination is that the cervical lymph nodes can be observed. Previous studies found that DECT-derived iodine content and overlay differ significantly among normal, inflammatory and metastatic squamous cell carcinoma cervical lymph nodes (11). However, there are still difficulties in locating cervical lymph nodes and the missed diagnosis of subclinical cervical LNM. Therefore, the main clinical significance of this study is that the clinical diagnosis of cervical LNM could also be implemented by analyzing the primary tumor of PTMC, even if the cervical LNM is not clear.

In this study, the metastasis rate of incomplete thyroid capsule in the LNM group (77.97%) was significantly higher than that in the non-LNM group (27.78%), and incomplete thyroid capsule had the highest correlation and diagnostic efficacy among morphological features. Its pathological mechanism is that PTMC may invade the thyroid capsule, and expand the contact area between the PTMC and lymphatic vessels and blood vessels, because it mostly occurs in the marginal region of the thyroid gland (12). The incidence of LNM in multiple lesions was higher than that in a single lesion (71.19% Vs 30.56%) in our study, which was consistent with the results of a study conducted by Zhao et al. (13). This result was associated with the spread of cancer tissue in the thyroid gland, and multiple lesions also increased the possibility of PTMC occurring at the thyroid marginal region which leads to an increased risk of LNM (14). In addition, LNM was more likely to occur when the maximum diameter was > 5 mm, and the aspect ratio > 1 of PTMC and metastasis rates increased by 30.14% and 31.97%, respectively. Several previous reports (15, 16) indicated that the maximum diameter was linearly related to the cervical LNM, and a maximum diameter > 5 mm can be used to predict metastasis and prognosis of PTMC, because the microvessels inside the larger PTMC are more abundant. The aspect ratio > 1 suggests that the PTMC grew in a noncircular shape and there is a possibility of multipolar invasive growth. When the PTMC showed incomplete nodule enhanced ring, the metastasis rate of the LNM group increased by 20.39% compared with the non-LNM group, indicating that PTMC broke through its own capsule and infiltrated the thyroid gland. Therefore, incomplete thyroid capsule, maximum diameter > 5.0 mm, irregular shape, and incomplete nodule enhanced ring could indicate that PTMC broke through the thyroid capsule and the tumor's own capsule, increasing the chance of PTMC contact with the surrounding capillary lymphatic vessels and the potential of cervical LNM. Further, combining incomplete thyroid capsule and maximum diameter can improve the diagnostic performance of LNM. In addition, we found that iodine image has an advantage over linear blending image in showing the structure of PTMC, especially the edge of the primary tumor. Surprisingly, the detection rate of microcalcification was low, and there was no correlation with LNM in the neck in this study, because the growth period of PTMC was short and there was less calcium deposition in infarcted tumor tissue and mucopolysaccharide calcification (17).

Compared with traditional morphological features, PTMC quantitative parameters of DECT are also significant for predicting cervical LNM. In this study, the results indicated that NICs and normalized CT values in arterial and venous phases had some value in predicting cervical LNM. Related research (18) showed that when the maximum diameter of PTMC was > 3 mm, the vascular density and tumor neovascularization were significantly increased, and

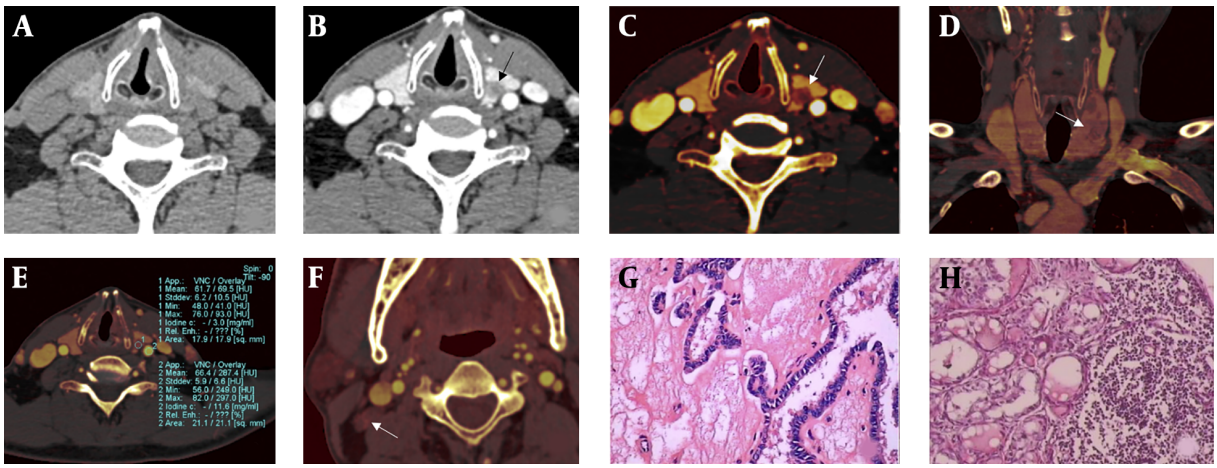

Figure 2. A 52-year-old male papillary thyroid microcarcinoma (PTMC) patient with lateral lymph node metastasis (LNM). The left lobe nodule of the thyroid was found after the health examination. Postoperative pathological results showed that the maximum diameter of the left PTMC with lateral LNM. Dual-energy linear blending image in non-enhanced CT images and arterial phase (A,B). Iodine images (C-F). Compared with the linear blending images, the boundary and internal structure of PTMC were clearer in the iodine image (black and white arrow in B, C). The iodine images show the left thyroid lobe's multiple noncircular low density lesions (white arrows in C, D). Incomplete thyroid capsule (white arrow in C), multiple lesion (white arrow in D), and normalized iodine concentration (NIC) of PTMC in arterial phase = 0.259 (E). All morphological features and quantitative parameters suggest that the thyroid nodules were malignant, and the cervical LNM potential was high. Image F shows a metastatic lymph node in the right area of the neck (white arrow). Postoperative pathological results showed that the maximum diameter of the left PTC was 7.0 mm (G, H&E staining, ×200) with lateral LNM (H, H&E staining, ×200).

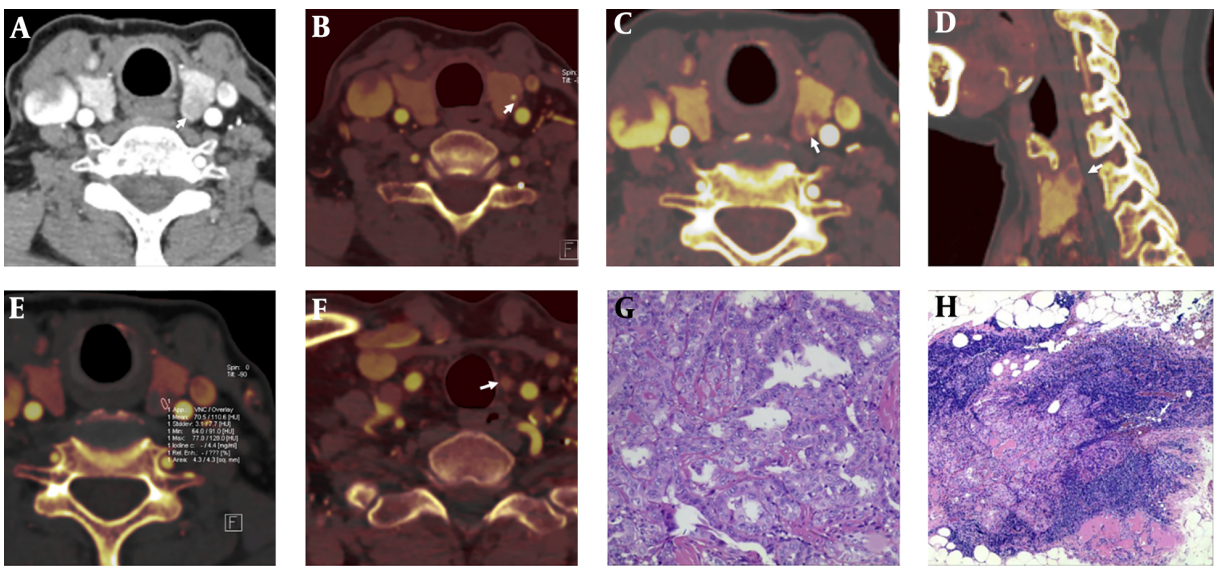

Figure 3. A 62-year-old female patient with papillary thyroid microcarcinoma (PTMC) and central lateral lymph node metastasis (LNM). PTMC was shown on dual-energy linear blending image in arterial phase (white arrow, A). Iodine images (B - F). PTMC with microcalcifications (white arrow, B). Incomplete nodule strengthening ring (white arrow, C). Incomplete thyroid capsule (white arrow, D). Normalized iodine concentration (NIC) of PTMC in arterial phase = 0.4 (E). The left central group LNM in the iodine image (white arrow, F). Postoperative pathological assessment shows PTMC and LNM (G,H); (H&E staining, ×100 and ×40, respectively).

the neovascular basement membrane was not well developed, leading to the larger vascular endothelium gap and the higher permeability. Therefore, blood flow was richer in larger-diameter PTMC, and the NIC and standardized CT values were higher, resulting in higher LNM metastatic potential. The ROC analysis showed that when the diagnostic threshold of NICROI in arterial phase was 0.208, the AUC was 0.814, which is the highest of the four quantitative parameters of iodine images. The sensitivity and specificity were 73.5% and 79.2%, respectively, which were better than

Table 1. Correlation Between Morphological Features in PTMC and Cervical LNM

Morphological features	PTMC with LNM		χ^2	P	r	P
	Negative (n = 36)	Positive (n = 59)				
Multiple lesion			14.965	< 0.001[b]	0.397	< 0.001[b]
Present	11 (30.56)	42 (71.19)				
Absent	25 (69.44)	17 (28.81)				
Maximum diameter, mm			8.724	0.004[b]	0.303	0.003[b]
> 5.0	16 (44.44)	44 (74.58)				
≤ 5.0	20 (55.56)	15 (25.42)				
Aspect ratio > 1			11.494	0.002[b]	0.348	0.001[b]
Present	19 (52.78)	50 (84.75)				
Absent	17 (47.22)	9 (15.25)				
Irregular shape			8.097	0.007[b]	0.309	0.004[b]
Present	20 (55.56)	41 (69.49)				
Absent	16 (44.44)	18 (30.51)				
Incomplete nodule enhanced ring			6.324	0.025[b]	0.258	0.012[b]
Present	25 (69.44)	53 (89.83)				
Absent	11 (30.56)	6 (10.17)				
Incomplete thyroid capsule			23.272	< 0.001[b]	0.495	< 0.001[b]
Present	10 (27.78)	46 (77.97)				
Absent	26 (72.22)	13 (22.03)				
Microcalcification			1.411	0.337	0.122	0.239
Present	7 (19.44)	18 (30.51)				
Absent	29 (80.56)	41 (69.49)				
Enhanced degree			1.475	0.242	0.119	0.229
Mild and moderate	26 (72.22)	27 (45.76)				
Significant	10 (27.78)	32 (54.24)				

Abbreviations: LNM, lymph node metastasis; PTMC, papillary thyroid microcarcinoma.
[a] Values are expressed as No. (%).
[b] Significance was considered when P < 0.05.

Table 2. Diagnosis Efficiency of Morphological Features in PTMC for Cervical LNM

Morphological features	Sensitivity, %	Specificity, %	Accuracy, %	AUC
Multiple lesion	71.10	69.40	70.50	0.703
Maximum diameter	74.50	55.60	67.40	0.595
Aspect ratio > 1	84.70	47.20	70.50	0.660
Irregular shape	69.49	44.44	60.00	0.570
Incomplete nodule enhanced ring	89.83	30.56	67.36	0.602
Incomplete thyroid capsule	77.97	72.22	75.79	0.757

Abbreviations: AUC, the area under the curve; LNM, lymph node metastasis; PTMC, papillary thyroid microcarcinoma.

those in the venous phase. The reason might be the arterial phase images showed more neovascularization branches of the tumors, with a high permeability. When normal follicular cells in PTMC were replaced by cancer cells and hyperplastic interstitial fibres, the iodine uptake capacity was reduced significantly, resulting in a lower IC (19). The growth of PTMC is mainly divided into two periods: slow growth without vascularization (pre-vascular phase) and

Table 3. Diagnosis Efficiency of Feature Combinations in PTMC for Cervical LNM

Feature combinations	Sensitivity, %	Specificity, %	Accuracy, %	AUC
A and B	94.92	55.56	80.00	0.752
A and C	93.22	55.56	78.95	0.744
A and D	93.22	52.78	77.89	0.730
A and E	93.22	63.89	82.11	0.786
A and F	94.92	38.89	73.68	0.669
B and C	96.61	44.44	76.84	0.705
B and D	89.83	44.44	72.63	0.671
B and E	93.22	38.89	72.63	0.661
B and F	93.22	36.11	71.58	0.647
C and D	88.14	41.67	70.53	0.649
C and E	91.53	47.22	74.74	0.694
C and F	91.53	33.33	69.47	0.624
D and E	91.53	38.89	71.58	0.652
D and F	91.53	41.67	72.63	0.666
E and F	93.22	36.11	71.58	0.647

Abbreviations: A, Incomplete thyroid capsule; AUC, the area under the curve; B, Multiple lesion; C, aspect ratio > 1; D, irregular shape; E, maximum diameter; F, incomplete nodule enhanced ring LNM, lymph node metastasis; PTMC, papillary thyroid microcarcinoma.

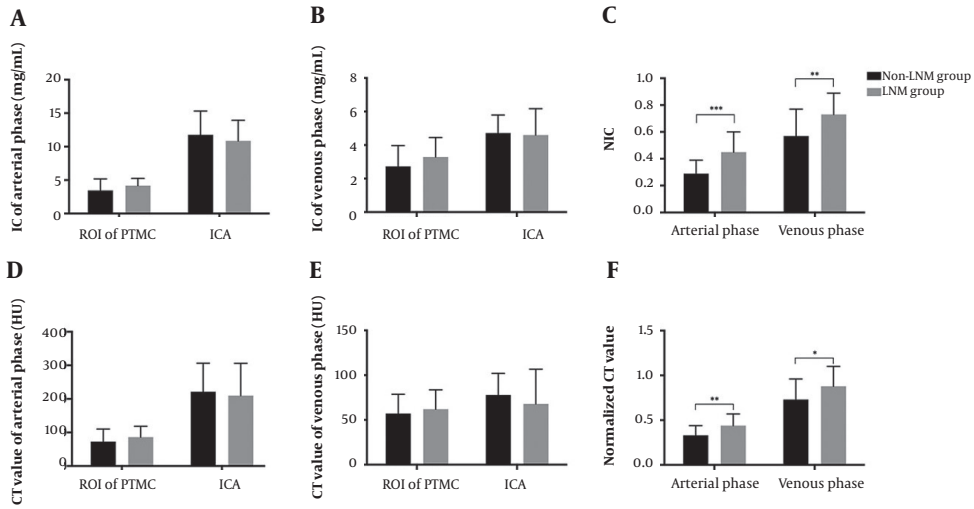

Figure 4. Iodine values and CT values in PTMC for prediction of cervical LNM. A and B, IC of PTMC and ICA in arterial and venous phases; C and F, Comparison between non-LNM group and LNM group in the NICs and normalized CT values. D and E, CT values of PTMC and ICA in arterial and venous phases. Bars mean standard deviation. *, Significance was considered when $P < 0.05$; **, significance was considered when $P < 0.01$; ***, significance was considered when $P < 0.001$. LNM, lymph node metastasis; IC, iodine concentration; ROI, region of interest; ICA, internal carotid artery; NIC, normalized iodine concentration. PTMC, papillary thyroid microcarcinoma.

rapid growth with a large number of neovascularizations (vascular phase). PTMC growth during the vascular phase is accelerated, so that LNM is more likely to occur during this period. Several studies have found that the LNM potential of PTMC was closely related to the density of lymphatic vessels and microvessels (20, 21). Further, when combining NICs in both arterial and venous phases, the diagnostic performance was improved compared with quantitative parameters alone. According to the results in this study, we should pay more attention to those PTMC patients with CT morphological features and quantitative parameters, especially incomplete thyroid capsule and NICROI, and then

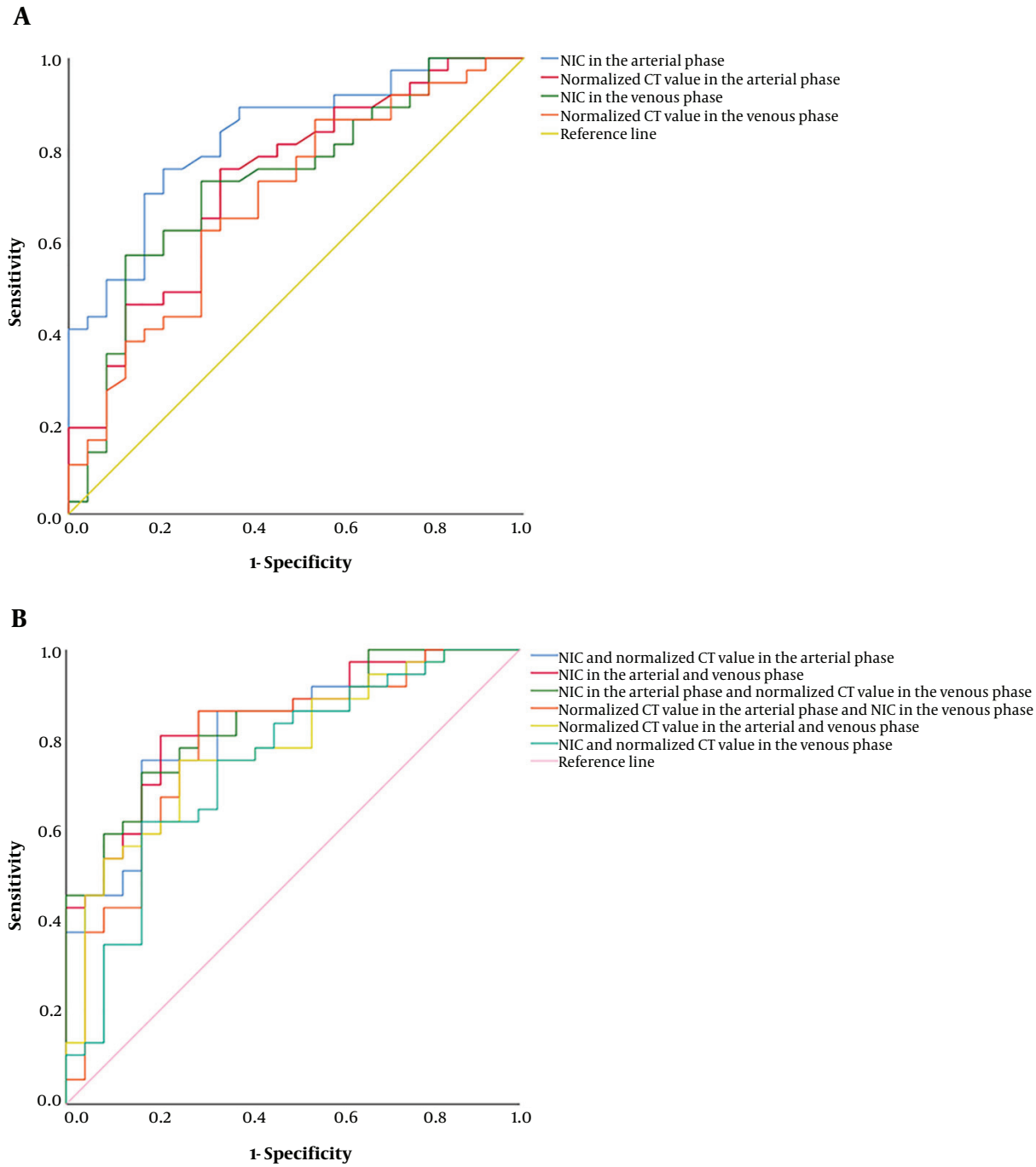

Figure 5. ROC (receiver operating characteristics) curves of iodine values and CT values for the diagnosis of lymph node metastasis (LNM) in patients with papillary thyroid microcarcinoma (PTMC). A, ROC comparison of normalized iodine concentration (NIC) in arterial phase, normalized CT value in arterial phase, NIC in venous phase, normalized CT value in venous phase; and B, Combinations of two parameters in the four significant iodine values and CT values.

carefully examine the neck for suspicious LNM.

The present study had some limitations. First, this retrospective study enrolled a limited number of pathologically confirmed PTMC cases with dual-energy CT examination of the neck, which is why univariate and multivariate logistic regression were not used to determine the

factors with a statistically significant effect on LNM. We would rather had used Spearman's rank correlation analysis. Thus, further studies with large samples are needed.

In conclusion, incomplete thyroid capsule and NIC of PTMC in the arterial phase could provide useful information in potential for cervical LNM. Furthermore, the combination of DECT parameters and morphological features of PTMC facilitates the discrimination of LNM and non-LNM, leading to more accurate diagnosis than using morphological features or quantitative parameters alone.

Footnotes

Authors' Contributions: Study concept and design: YLH and DH. Acquisition of data: YLH, YMJ, and ZHZ. Analysis and interpretation of data: WZ, YJ, and BH. Statistical analysis and drafting of the manuscript: YLH, YMJ, and DH. Technical support: YL.

Conflict of Interests: All authors declare there is no conflict of interest.

Ethical Approval: This research was carried out in accordance with the ethical standards of our Institutional Committee.

Funding/Support: This study received Basic Research Program of Yunnan Province (Joint Special Project of Kunming Medical University) (code1: 2019FE001(-213)).

Informed Consent: This was a retrospective, single-center study approved by our institutional review board, and the requirement for informed written consent was waived.

References

1. Hedinger C, Williams ED, Sobin LH. The WHO histological classification of thyroid tumors: A commentary on the second edition. *Cancer*. 1989;**63**(5):908–11. doi: 10.1002/1097-0142(19890301)63:5<908::aid-cncr2820630520>3.0.co;2-i. [PubMed: 2914297].
2. Pacini F. Management of papillary thyroid microcarcinoma: Primum non nocere!. *J Clin Endocrinol Metab*. 2013;**98**(4):1391–3. doi: 10.1210/jc.2013-1634. [PubMed: 23564944].
3. Zhang L, Wei WJ, Ji QH, Zhu YX, Wang ZY, Wang Y, et al. Risk factors for neck nodal metastasis in papillary thyroid microcarcinoma: A study of 1066 patients. *J Clin Endocrinol Metab*. 2012;**97**(4):1250–7. doi: 10.1210/jc.2011-1546. [PubMed: 22319042].
4. Pitoia F, Miyauchi A. 2015 American Thyroid Association Guidelines for Thyroid Nodules and Differentiated thyroid cancer and their implementation in various care settings. *Thyroid*. 2016;**26**(2):319–21. doi: 10.1089/thy.2015.0530. [PubMed: 26576627].
5. Haugen BR, Alexander EK, Bible KC, Doherty GM, Mandel SJ, Nikiforov YE, et al. 2015 American Thyroid Association Management Guidelines for adult patients with thyroid nodules and differentiated thyroid cancer: The American Thyroid Association Guidelines task force on thyroid nodules and differentiated thyroid cancer. *Thyroid*. 2016;**26**(1):1–133. doi: 10.1089/thy.2015.0020. [PubMed: 26462967]. [PubMed Central: PMC4739132].
6. Luo Y, Zhao Y, Chen K, Shen J, Shi J, Lu S, et al. Clinical analysis of cervical lymph node metastasis risk factors in patients with papillary thyroid microcarcinoma. *J Endocrinol Invest*. 2019;**42**(2):227–36. doi: 10.1007/s40618-018-0908-y. [PubMed: 29876836]. [PubMed Central: PMC6394766].
7. Xu Y, Xu L, Wang J. Clinical predictors of lymph node metastasis and survival rate in papillary thyroid microcarcinoma: Analysis of 3607 patients at a single institution. *J Surg Res*. 2018;**221**:128–34. doi: 10.1016/j.jss.2017.08.007. [PubMed: 29229118].
8. Fulwadhva UP, Wortman JR, Sodickson AD. Use of dual-energy CT and iodine maps in evaluation of bowel disease. *Radiographics*. 2016;**36**(2):393–406. doi: 10.1148/rg.2016150151. [PubMed: 26963452].
9. Li M, Zheng X, Li J, Yang Y, Lu C, Xu H, et al. Dual-energy computed tomography imaging of thyroid nodule specimens: Comparison with pathologic findings. *Invest Radiol*. 2012;**47**(1):58–64. doi: 10.1097/RLI.0b013e318229fef3. [PubMed: 21788907].
10. Liu Z, Lv X, Wang W, An J, Duan F, Feng X, et al. Imaging characteristics of primary intracranial teratoma. *Acta Radiol*. 2014;**55**(7):874–81. doi: 10.1177/0284185113507824. [PubMed: 24103916].
11. Tawfik AM, Razek AA, Kerl JM, Nour-Eldin NE, Bauer R, Vogl TJ. Comparison of dual-energy CT-derived iodine content and iodine overlay of normal, inflammatory and metastatic squamous cell carcinoma cervical lymph nodes. *Eur Radiol*. 2014;**24**(3):574–80. doi: 10.1007/s00330-013-3035-3. [PubMed: 24081649].
12. Han ZJ, Shu YY, Lai XF, Chen WH. Value of computed tomography in determining the nature of papillary thyroid microcarcinomas: Evaluation of the computed tomographic characteristics. *Clin Imaging*. 2013;**37**(4):664–8. doi: 10.1016/j.clinimag.2012.12.005. [PubMed: 23462729].
13. Zhao Q, Ming J, Liu C, Shi L, Xu X, Nie X, et al. Multifocality and total tumor diameter predict central neck lymph node metastases in papillary thyroid microcarcinoma. *Ann Surg Oncol*. 2013;**20**(3):746–52. doi: 10.1245/s10434-012-2654-2. [PubMed: 22972508].
14. Jovanovic L, Delahunt B, McIver B, Eberhardt NL, Bhattacharya A, Lea R, et al. Distinct genetic changes characterise multifocality and diverse histological subtypes in papillary thyroid carcinoma. *Pathology*. 2010;**42**(6):524–33. doi: 10.3109/00313025.2010.508780. [PubMed: 20854070].
15. Lim YC, Choi EC, Yoon YH, Kim EH, Koo BS. Central lymph node metastases in unilateral papillary thyroid microcarcinoma. *Br J Surg*. 2009;**96**(3):253–7. doi: 10.1002/bjs.6484. [PubMed: 19224514].
16. Mercante G, Frasoldati A, Pedroni C, Formisano D, Renna L, Piana S, et al. Prognostic factors affecting neck lymph node recurrence and distant metastasis in papillary microcarcinoma of the thyroid: Results of a study in 445 patients. *Thyroid*. 2009;**19**(7):707–16. doi: 10.1089/thy.2008.0270. [PubMed: 19348581].
17. Khoo ML, Asa SL, Witterick IJ, Freeman JL. Thyroid calcification and its association with thyroid carcinoma. *Head Neck*. 2002;**24**(7):651–5. doi: 10.1002/hed.10115. [PubMed: 12112538].
18. Chen Z, Wu L, Lu L, Yang G. Quantitative parameters in iodine overlay image based on dual-source dual-energy computed tomography in differentiating benign and malignant thyroid nodules. *Chin J Radiol*. 2015;**49**(6):646–50.
19. Capp C, Wajner SM, Siqueira DR, Brasil BA, Meurer L, Maia AL. Increased expression of vascular endothelial growth factor and its receptors, VEGFR-1 and VEGFR-2, in medullary thyroid carcinoma. *Thyroid*. 2010;**20**(8):863–71. doi: 10.1089/thy.2009.0417. [PubMed: 20615131].
20. Pereira F, Pereira SS, Mesquita M, Morais T, Costa MM, Quelhas P, et al. Lymph node metastases in papillary and medullary thyroid carcinoma are independent of intratumoral lymphatic vessel density. *Eur Thyroid J*. 2017;**6**(2):57–64. doi: 10.1159/000457794. [PubMed: 28589086]. [PubMed Central: PMC5422756].
21. Folkman J. What is the evidence that tumors are angiogenesis dependent? *J Natl Cancer Inst*. 1990;**82**(1):4–6. doi: 10.1093/jnci/82.1.4. [PubMed: 1688381].